Thompson Jobe, J.A., Li, T., Bookhagen, B., Chen, J., and Burbank, D., 2018, Dating growth strata and basin fill by combining $^{26}Al/^{10}Be$ burial dating and magnetostratigraphy: Constraining active deformation in the Pamir–Tian Shan convergence zone, NW China: Lithosphere, https://doi.org/10.1130/L727.1.

GSA DATA REPOSITORY ITEM 2018311

Calculation of Post-burial Production

Post-burial production includes topographic and depth shielding and assumes a rock density of 2.65 g/cm^3. We assume all samples were well shielded (>30 m of overburden) until a certain time in the recent past, at which point we assume instantaneous incision down to the present-day level.

Topographic and self-shielding were calculated using CosmoCalc 2.1 (Vermeesch 2007). Production rates for samples at depth were calculated using sea level high latitude production rates of 4.63 and 31.1 g/atom/yr for ^{10}Be and ^{26}Al, respectively (Granger and Muzikar, 2001; Balco et al., 2008), scaled to each site and described in main text.

To calculate the post burial production, we followed equations 1-4 in the main text, where z was the depth of incision from the known terrace surface or the calculated nominal shielding depth (below). In the second term of equations 1 and 2, t is the since abandonment of the surface, i.e., the terrace age, from optically stimulated luminescence and cosmogenic depth profile dating of the terrace surfaces. We calculated the amount of production for a sample buried at a depth, z, for time t, following the Monte Carlo techniques outlined the main text, and subtracted this concentration from measured ^{10}Be and ^{26}Al concentrations to remove the effect of the recent production. We then calculated a corrected $^{26}Al/^{10}Be$ ratio and burial age.

Nominal shielding was calculated for MING, SWMG, and PBB-2. For each site, we calculated the angle from the sample to the skyline across the incised valley ($\alpha_{horizon}$). We subtracted this angle from 90° to calculate the angle of open sky above the sample ($\alpha_{opensky}$). This open sky angle is then divided by 2, and added to the $\alpha_{horizon}$ to determine α_{sample}, the midway point between the shielded horizon and the shielding from the cliff above the sample. The α_{sample} is used, in conjunction with the width of the overhang from which the sample was collected, to calculate the nominal shielding. These calculations are only used to determine the present-day nominal shielding.

At Mingyaole (MING) (Figure DR1), the terrace across the incised valley is ~30 m above the modern river level, leading to a $\alpha_{horizon}$ of 45°, and leaving 45° of the sky open ($\alpha_{opensky}$). Dividing $\alpha_{opensky}$ by 2 and adding it to $\alpha_{horizon}$ yields an angle of ~68°. Using the overhang width of 3.5 m, we calculate a nominal shielding of ~9.3 m since 15 ka.

At southwest Mingyaole (SWMG) (Figure DR6), the terrace across the incised valley is ~50 m above the modern river level, leading to a $\alpha_{horizon}$ of 8°, and leaving 82° of the sky open ($\alpha_{opensky}$). Dividing $\alpha_{opensky}$ by 2 and adding it to $\alpha_{horizon}$ yields an angle of ~41°. Using the overhang width of 4.5 m, we calculate a nominal shielding of ~5 m since 15 ka.

At PBB-2, nominal shielding was estimated from the width of the overhang and the angle open to the sky under the larger overhang (~70°, height of overhang = 46 m, Figure 5d). Given the irregular shape of the bowl, we chose an "average" nominal shielding depth based on the angle of ~70° and the width of the smaller overhang (~2 m). These calculations yield a nominal shielding depth of ~6 m.

References

Balco, G., Stone, J. O., Lifton, N. A., Dunai, T. J., 2008. A complete and easily accessible means of calculating surface exposure ages or erosion rates form ^{10}Be and ^{26}Al measurements. Quaternary Geochronology 3, 174-195.

Granger, D., P. F. Muzikar. 2001. Dating sediment burial with in situ-produced cosmogenic nuclides: theory, techniques, and limitations. Earth and Planetary Science Letters, 188: 269-281.

Vermeesch, P., 2007. CosmoCalc: An Excel add-in for cosmogenic nuclide calculations. Geochemistry, Geophysics, Geosystems 8 Q08003, doi:10.1029/2006GC001530.

TABLE DR1. POST BURIAL PRODUCTION

Sample	^{10}Be (10^4 atoms g^{-1})	^{26}Al (10^4 atoms g^{-1})	Corrected $^{26}Al/^{10}Be$ ratio	Corrected $^{26}Al/^{10}Be$ Age
MING	0.02 ± 0.004	0.19 ± 0.03	$4.8^{+2.0}/_{-2.1}$	$0.9^{+1.1}/_{-0.7}$
MSN	0.23 ± 0.003	2.1 ± 0.3		$2.1^{+2.1}/_{-1.2}$
ATSH	0.11 ± 0.002	0.92 ± 0.15	$0.97^{+0.9}/_{-0.7}$	$3.8^{+2.1}/_{-1.3}$
SWMG	0.25 ± 0.004	2.13 ± 0.37	$2.7^{+2.2}/_{-1.7}$	$1.7^{+1.7}/_{-0.8}$

TABLE DR2. $^{26}AL/^{27}AL$ MEASUREMENTS MADE AT PRIME AND LLNL

Sample	PRIME			LLNL		
	$^{26}Al/^{27}Al$ ratio (10^{-15}) *,†	$^{26}Al/^{27}Al$ ratio error (10^{-15}) *,†	% error	$^{26}Al/^{27}Al$ ratio (10^{-15}) *,†	$^{26}Al/^{27}Al$ ratio error (10^{-15}) *,†	% error
PBB-1	4.0	12.4	3.1	10	5.16	0.52
PBB-2	1.0	21.7	21.7	8.1	5.83	0.72
OYT	1.0	22.7	22.7	22	7.94	0.36
MING	79.0	36.0	0.46			
WATSH	1.0	286.1	286			
MSN	18.0	55.7	3.1	69.7	15.3	0.22
ATSH	4.0	14.7	3.68			
SWMG	19.0	13.9	0.73			

* Isotope ratios were normalized to ^{26}Al standards prepared by Nishiizumi et al. (2007) and a ^{26}Al half-life of 0.7 x 10^6 years.
† $^{26}Al/^{27}Al$ ratios were corrected using a laboratory blank (n=2) of 4.09 x 10^{-15} for samples PBB-1 and PBB-2, and 0 x 10^{-15} for MING, SWMG, ATSH, WATSH, OYT, and MSN.

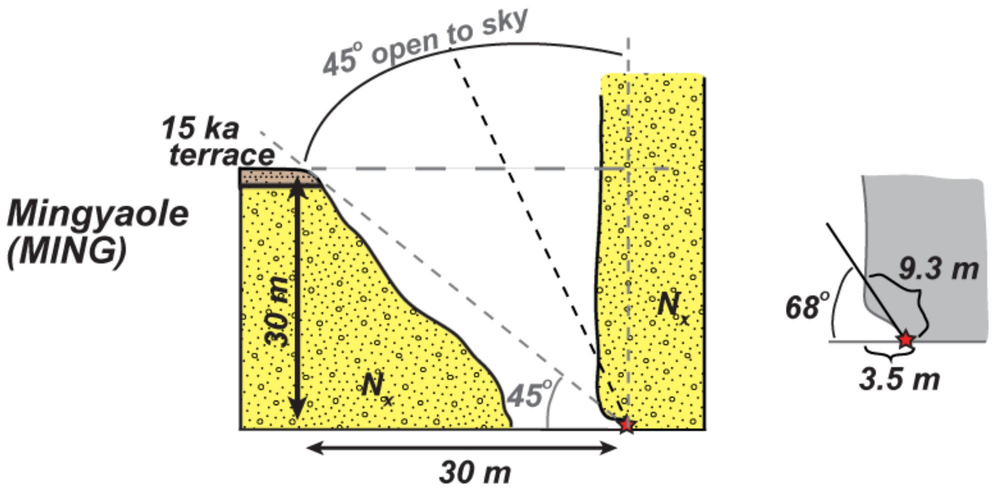

Figure DR1. Schematic site illustration showing the shielding of the Mingyaole burial dating site and nominal shielding. Nx – Xiyu Formation (Plio-Pleistocene conglomerates); brown stippled units, with ages, are Late Quaternary fluvial terraces. Ages based on OSL dating and regional terrace correlation (see text). Red star marks location of burial sample. No vertical exaggeration.

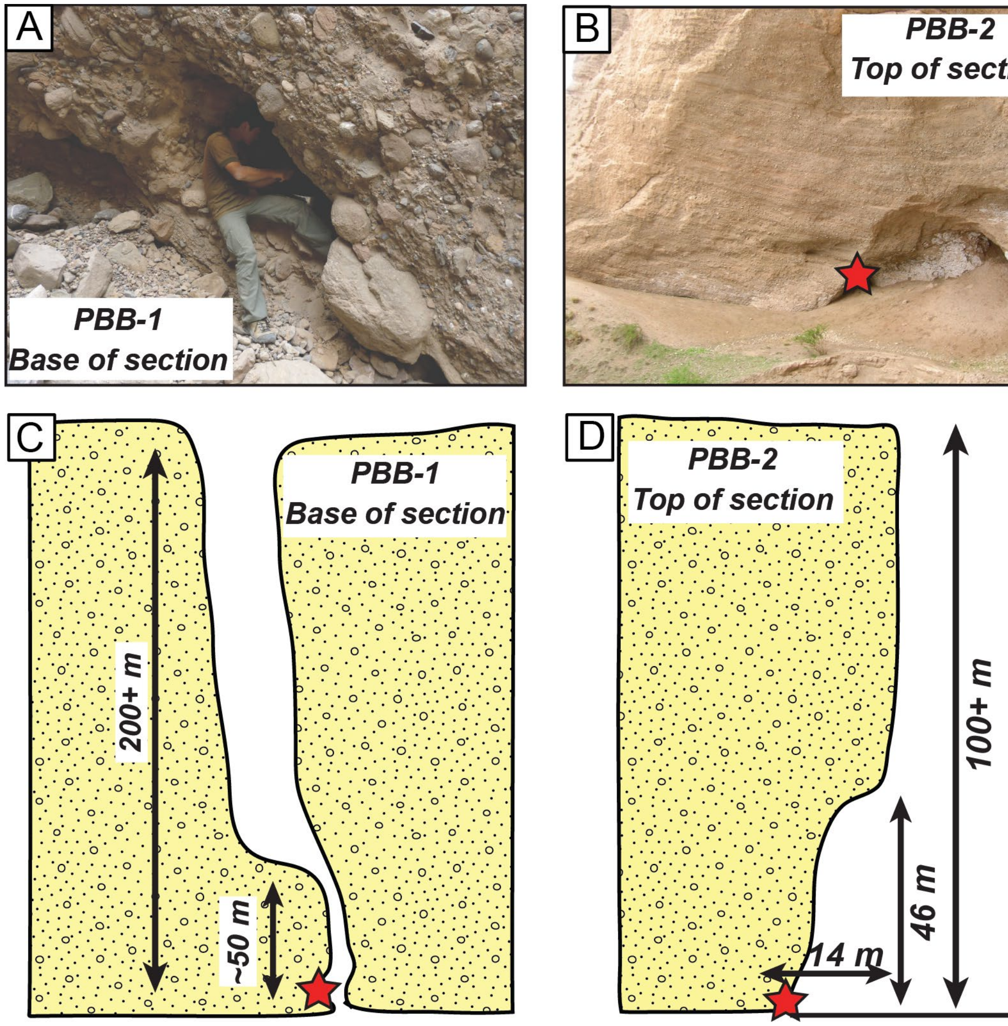

Figure DR2. Field photos of the (A) PBB-1 and (B) PBB-2 sample sites. Schematic site illustration showing the shielding and burial of the (C) PBB-1 and (D) PBB-2 sample sites. Red star marks location of burial sample.

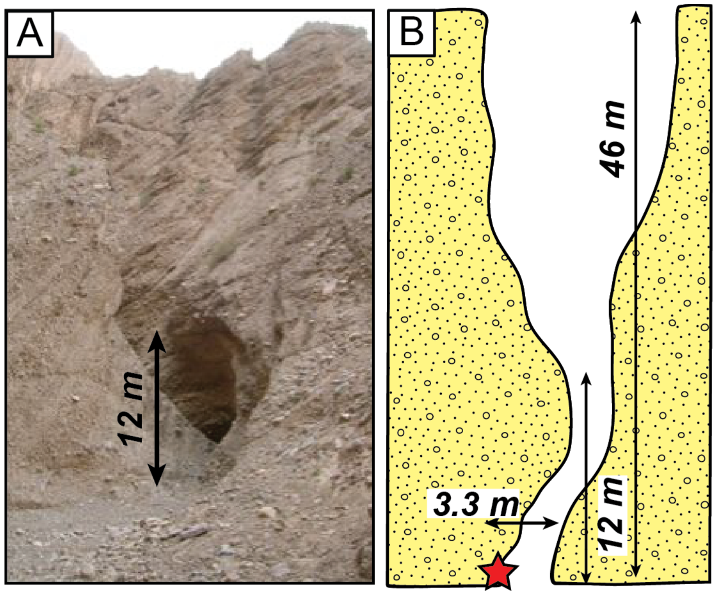

Figure DR3. (A) Field photo of the Kelatuo anticline sample site. (B) Schematic site illustration showing the shielding and burial of the Kelatuo anticline sample site. Red star marks location of burial sample.

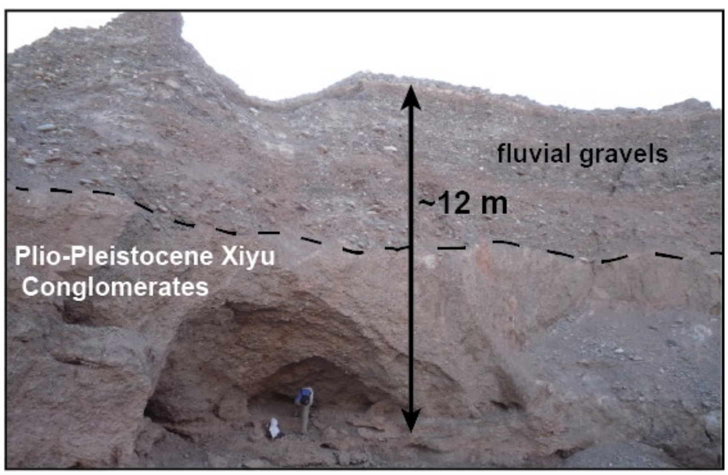

Figure DR4. Field photo of the Mushi anticline sample site.

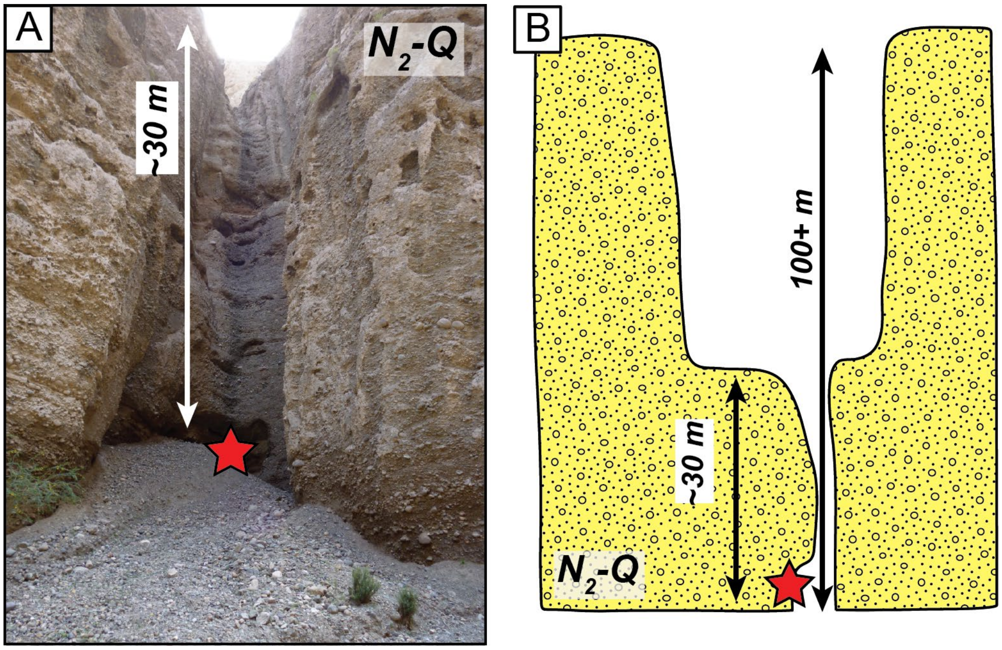

Figure DR5. (A) Field photo of the Oytag sample site. (B) Schematic site illustration showing the shielding and burial of the Oytag sample site. Red star marks location of burial sample.

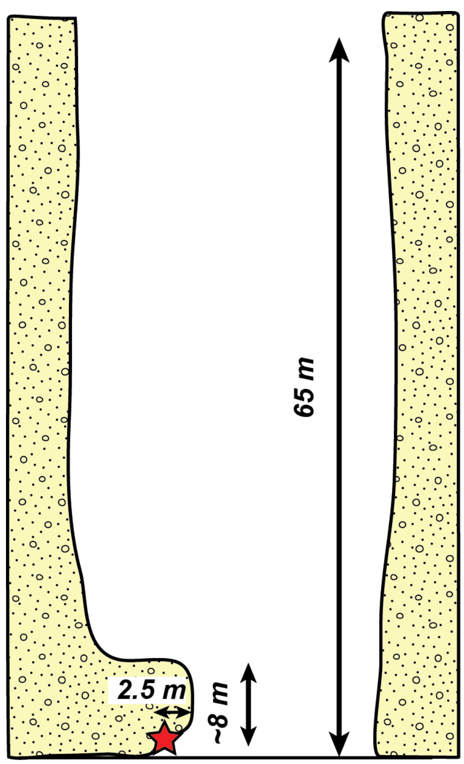

Figure DR6. Schematic sketch of the Atushi sample site. Red star marks location of burial sample.

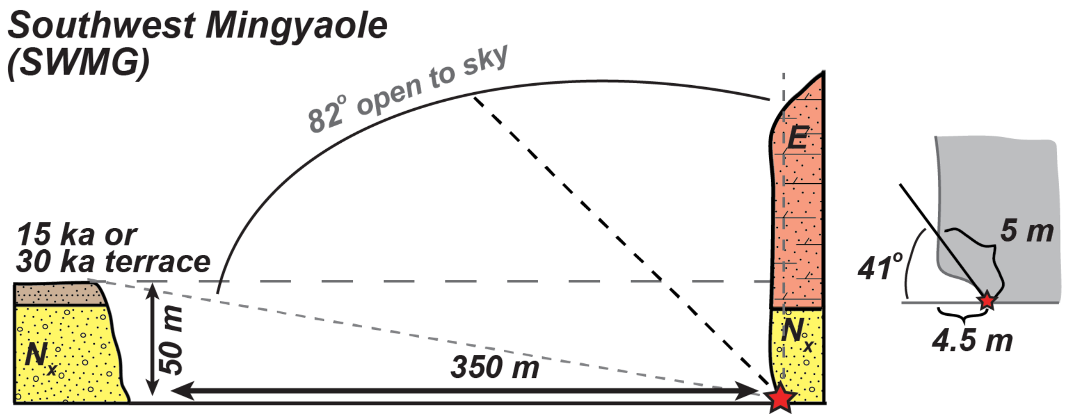

Figure DR7. Schematic site illustration showing the shielding of the Southwest Mingyaole sample site and parameters used for nominal shielding calculation. Nx – Xiyu Formation (Plio-Pleistocene conglomerates); E – Paleogene; brown stippled units, with ages, are Late Quaternary fluvial terraces. Ages based on OSL dating and regional terrace correlation (see text). Red star marks location of burial sample. No vertical exaggeration.